

Heating, Energetic Particle Confinement and Transport in Quasi-Omnigenous Stellarators

US /Japan Workshop on Stellarator/Helical System Concept Improvement
September 23-24, 1999
Oak Ridge National Laboratory

D. A. Spong, S. P. Hirshman, D. B. Batchelor, L. A. Berry,
J. Carlsson, J. F. Lyon

Oak Ridge National Laboratory
Oak Ridge, TN 37831-8071



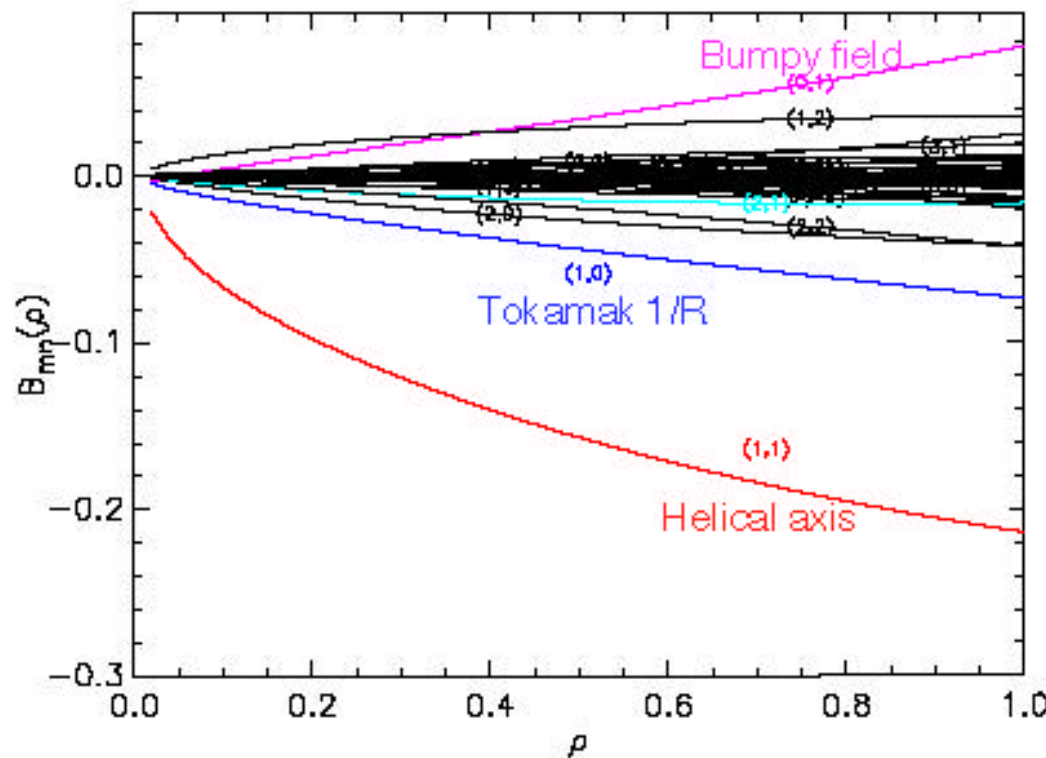
Overview and Motivations

- Goals of the QOS (Quasi-Omnigenous) approach
 - Extension of advanced stellarator physics to low aspect ratio
 - While maintaining good confinement/stability properties
 - Low plasma currents: most of transform comes from coils
- Confinement improvement has been central to QO optimization process
 - uses simple, rapidly evaluated transport criteria
 - $J^*(\cdot)$, $B_{min}(\cdot)$, $B_{max}(\cdot)$
- Tool development (in parallel with evaluation of new QO configurations)
 - core neoclassical transport
 - Particle simulation (DELTA5D)
 - Drift Kinetic Equation solution (DKES)
 - confinement analysis of energetic tail populations
 - ICRF heated ions, alphas, neutral beams
 - Bootstrap current
 - f method. DKES

Typical QOS B_{mn} spectra show that the helical component is dominant. The $1/R$ term is down from its axisymmetric tokamak level about a factor of 4.

$$N_{fp} = 3, R_0/\langle a \rangle = 3.6$$

Note: $B_{0,0} = 1$

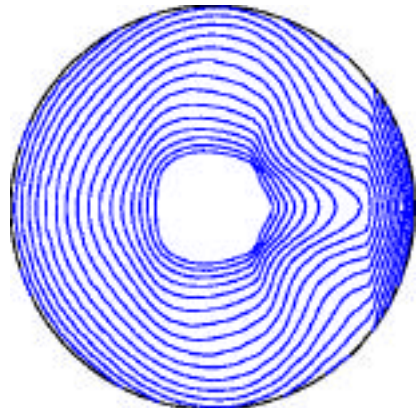


This spectrum differs significantly from that of either HSX or W7-X.

QOS Devices achieve good transport by targeting closed J^* , B_{\min} , and B_{\max} surfaces at low aspect ratio.

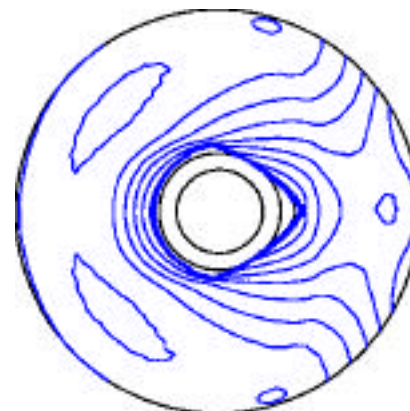
QO transport is driven by deviations from $J^* = J^*(\psi)$ and open J^* surfaces in transitional region

Deeply trapped



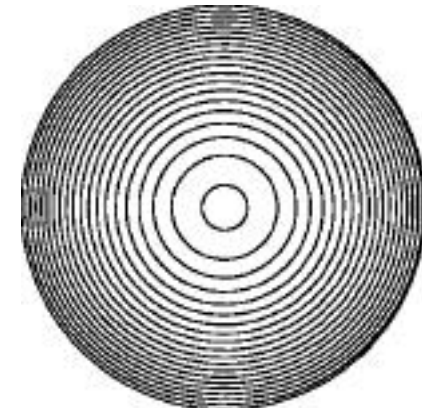
$\beta/\mu = 0.95$ Tesla

Transitional



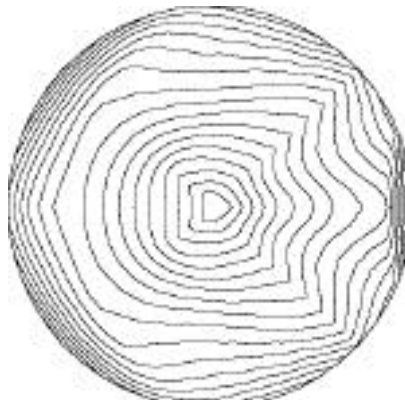
$\beta/\mu = 1.09$ Tesla

Passing

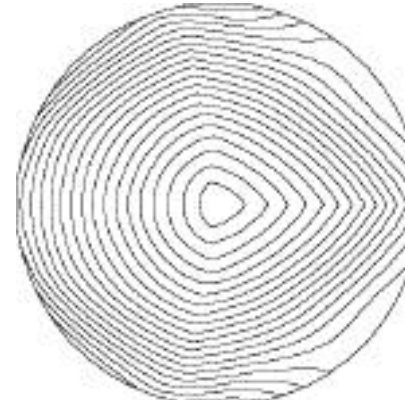


$\beta/\mu = 1.5$ Tesla

B_{\min}



B_{\max}



Tools used in the analysis of QO configurations:

- Coil generation: COILOPT
- 3D equilibrium: VMEC
- Transport, confinement
 - DELTA5D (Stellarator Particle Simulation Code)
 - DKES (Drift Kinetic Equation Solver)
 - SYMPORBIT (symplectic orbit integrator)
 - J^* , J , B_{\min} , B_{\max} contour plotting
- Stability
 - COBRA (fast matrix/variational 3D ballooning, R. Sanchez)
 - Terpsichore - Kink instabilities (R. Sanchez)
 - Resistive MHD for 3D configurations (L. Garcia)
- Bootstrap Current
 - Tolliver/Berry code (collisionless limit), NIFS multi-regime code
 - Particle based f calculation using DELTA5D
 - DKES (Drift Kinetic Equation Solver)

The DKES (Drift Kinetic Equation Solver) provides the full neoclassical transport coefficient matrix (multi-helicity)

$$\vec{Q} \cdot \vec{s} = -\frac{3}{2} \frac{T}{n} - \frac{eE_r}{T}$$

$$I_i = \frac{1}{T} \bar{Q} \cdot \vec{s} = -\sum_{j=1}^3 L_{ij} A_j \quad A_j = \frac{T}{T}$$

$$n \langle (\vec{u} - \vec{u}_s) \cdot \vec{B} \rangle - \frac{e}{T} \frac{\langle \vec{E} \cdot \vec{B} \rangle}{\langle B^2 \rangle}$$

$$L_{ij} = n \frac{2}{\sqrt{\int_0^r}} dK \sqrt{K} e^{-K} g_i g_j D_{ij}$$

$$\text{where } g_1 = g_3 = 1, \quad g_2 = K, \quad K = \frac{v}{v_{th}}$$

$$D_{11} = D_{12} = D_{21} = D_{22} = -\frac{v_{th}}{2} \frac{B v_{th}}{d} \frac{d}{dr}^{-1} K \sqrt{K}_{11}$$

$$D_{31} = D_{32} = -D_{13} = -D_{23} = -\frac{v_{th}}{2} \frac{B v_{th}}{d} \frac{d}{dr}^{-1} K_{31}$$

$$D_{33} = -\frac{v_{th}}{2} \sqrt{K}_{33}$$

$$L_{ij} = \frac{g_i}{v} \frac{E_r}{v}$$

(i.e., to carry out the above integrals, one will need to generate a 2-D matrix of 's vs. these parameters for each flux surface)

Recently, optimized spectra have been developed for QOS DKES calculations (ref. W. Van Rij, S. Hirshman, H. Massberg)

- Uses recurrence relation based on the convolution of $\| \ln B^{-1}$ with the perturbed distribution function: $S_n = S S_{n-1} + S S_{n-1}$
- S = dependent spectra associated with $B^{-1}/$
- $S - S$ spectra associated with $B^{-1}/$

Earlier spectrum

N	M = 0	1	2	3	4	5	6	7	8	9	10	11	12	13	14
0	0	1	2	3	4	5	6	7	8	9	10	11	12	13	14
1	0	1	2	3	4	5	6	7	8	9	10	11	12	13	14
2	0	1	2	3	4	5	6	7	8	9	10	11	12	13	14
3	0	1	2	3	4	5	6	7	8	9	10	11	12	13	14
4	0	1	2	3	4	5	6	7	8	9	10	11	12	13	14
5	0	1	2	3	4	5	6	7	8	9	10	11	12	13	14
6	0	1	2	3	4	5	6	7	8	9	10	11	12	13	14
7	0	1	2	3	4	5	6	7	8	9	10	11	12	13	14
-1	0	1	2	3	4	5	6	7	8	9	10	11	12	13	14
-2	0	1	2	3	4	5	6	7	8	9	10	11	12	13	14
-3	0	1	2	3	4	5	6	7	8	9	10	11	12	13	14
-4	0	1	2	3	4	5	6	7	8	9	10	11	12	13	14
-5	0	1	2	3	4	5	6	7	8	9	10	11	12	13	14
-6	0	1	2	3	4	5	6	7	8	9	10	11	12	13	14
-7	0	1	2	3	4	5	6	7	8	9	10	11	12	13	14
-8	0	1	2	3	4	5	6	7	8	9	10	11	12	13	14
-9	0	1	2	3	4	5	6	7	8	9	10	11	12	13	14
-10	0	1	2	3	4	5	6	7	8	9	10	11	12	13	14
-11	0	1	2	3	4	5	6	7	8	9	10	11	12	13	14
-12	0	1	2	3	4	5	6	7	8	9	10	11	12	13	14
-13	0	1	2	3	4	5	6	7	8	9	10	11	12	13	14
-14	0	1	2	3	4	5	6	7	8	9	10	11	12	13	14
-15	0	1	2	3	4	5	6	7	8	9	10	11	12	13	14
8	0	1	2	3	4	5	6	7	8	9	10	11	12	13	14
9	0	1	2	3	4	5	6	7	8	9	10	11	12	13	14
10	0	1	2	3	4	5	6	7	8	9	10	11	12	13	14
11	0	1	2	3	4	5	6	7	8	9	10	11	12	13	14
12	0	1	2	3	4	5	6	7	8	9	10	11	12	13	14
13	0	1	2	3	4	5	6	7	8	9	10	11	12	13	14
14	0	1	2	3	4	5	6	7	8	9	10	11	12	13	14
15	0	1	2	3	4	5	6	7	8	9	10	11	12	13	14

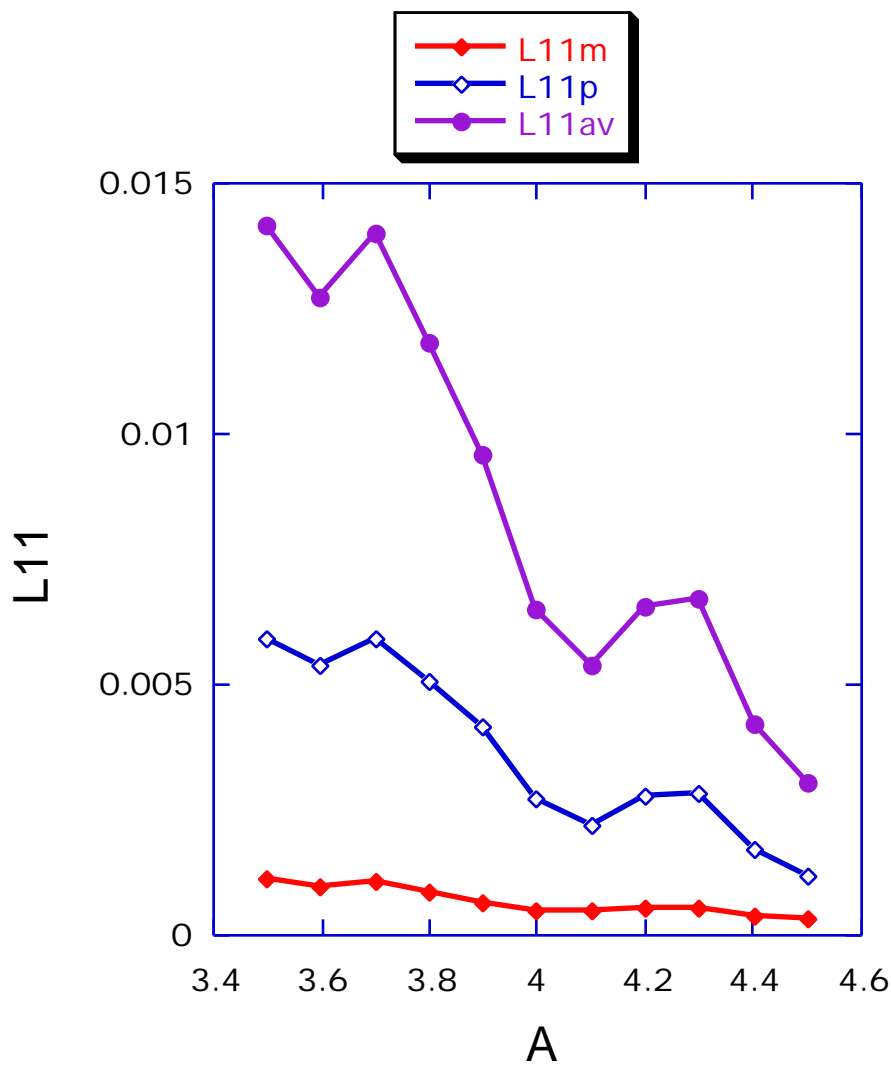
N	M = 1	M = 2	M = 3	M = 4	M = 5	M = 6	M = 7	M = 8	M = 9	M = 10	M = 11	M = 12	M = 13	M = 14	M = 15	M = 16	M = 17	M = 18	M = 19
-17	1																		
-16	1																		
-15	1	2																	
-14	1	2	3																
-13	1	2	3	4															
-12	1	2	3	4	5														
-11	1	2	3	4	5	6													
-10	1	2	3	4	5	6	7												
-9	1	2	3	4	5	6	7	8											
-8	1	2	3	4	5	6	7	8	9										
-7	1	2	3	4	5	6	7	8	9	10									
-6	1	2	3	4	5	6	7	8	9	10	11								
-5	1	2	3	4	5	6	7	8	9	10	11	12							
-4	1	2	3	4	5	6	7	8	9	10	11	12	13						
-3	1	2	3	4	5	6	7	8	9	10	11	12	13	14					
-2	1	2	3	4	5	6	7	8	9	10	11	12	13	14	15				
-1	1	2	3	4	5	6	7	8	9	10	11	12	13	14	15	16			
0	0	1	2	3	4	5	6	7	8	9	10	11	12	13	14	15	16	17	
1	0	1	2	3	4	5	6	7	8	9	10	11	12	13	14	15	16	17	18
2	0	1	2	3	4	5	6	7	8	9	10	11	12	13	14	15	16	17	18
3	0	1	2	3	4	5	6	7	8	9	10	11	12	13	14	15	16	17	18
4	0	1	2	3	4	5	6	7	8	9	10	11	12	13	14	15	16	17	18
5	0	1	2	3	4	5	6	7	8	9	10	11	12	13	14	15	16	17	18
6	0	1	2	3	4	5	6	7	8	9	10	11	12	13	14	15	16	17	18
7	0	1	2	3	4	5	6	7	8	9	10	11	12	13	14	15	16	17	18
8	0	1	2	3	4	5	6	7	8	9	10	11	12	13	14	15	16	17	18
9	0	1	2	3	4	5	6	7	8	9	10	11	12	13	14	15	16	17	18
10	0	1	2	3	4	5	6	7	8	9	10	11	12	13	14	15	16	17	18
11	0	1	2	3	4	5	6	7	8	9	10	11	12	13	14	15	16	17	18
12	0	1	2	3	4	5	6	7	8	9	10	11	12	13	14	15	16	17	18
13	0	1	2	3	4	5	6	7	8	9	10	11	12	13	14	15	16	17	18
14	0	1	2	3	4	5	6	7	8	9	10	11	12	13	14	15	16	17	18
15	0	1	2	3	4	5	6	7	8	9	10	11	12	13	14	15	16	17	18

Optimized spectrum

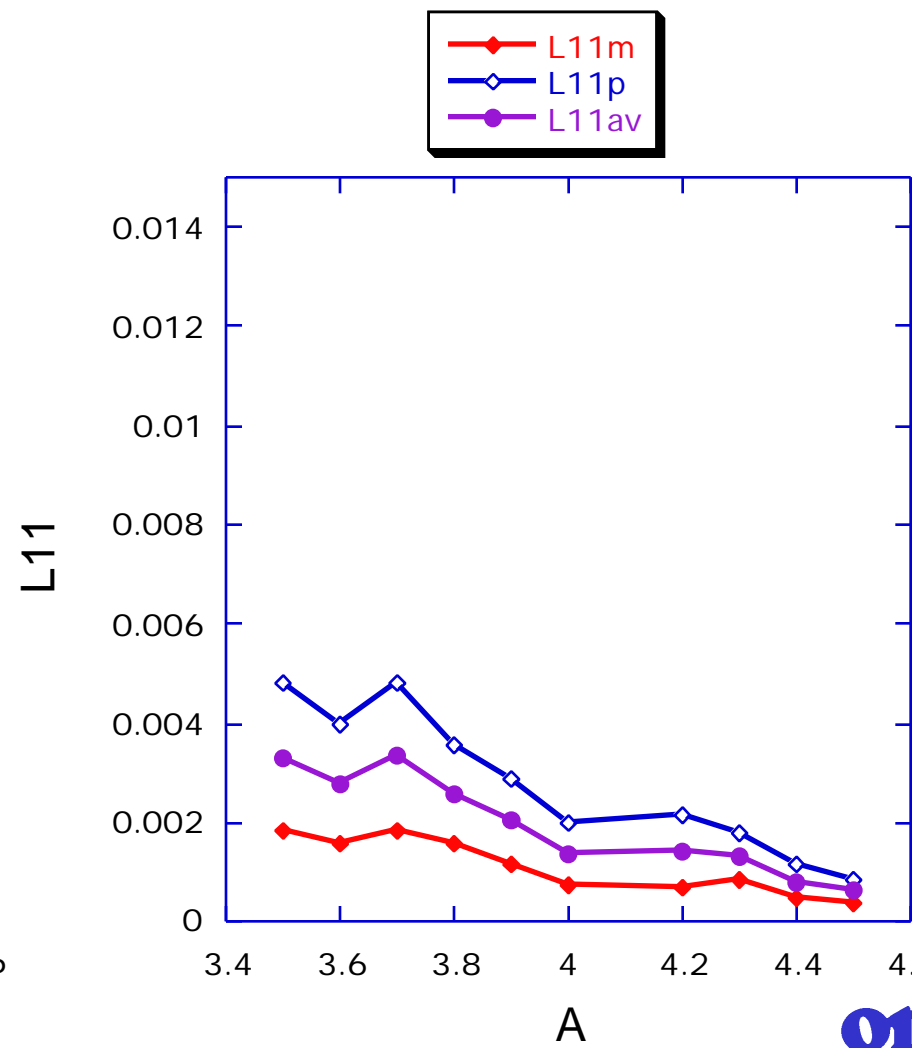


Using the new spectra, tighter upper and lower bounds are obtained on QOS transport coefficients without increasing the number of modes

Rectangular m,n spectrum



Optimized m,n spectrum



Applications of DKES to QO transport:

- Collisional bootstrap current
- Ambipolarity studies
 - Initially, use DKES for both electron and ion fluxes
 - Then hybrid model: DKES electron flux with ion particle flux from particle-based calculation
- Use in the optimizer with a truncated set of modes
- Viscous stress tensor
- Couple to 1-1/2D fluid transport codes

DELTA5D Particle simulation code is used for both thermal plasma ion transport and fast ion confinement studies

- Thermal plasma
 - Local diffusive and direct losses
outgrowth of Fowler, Rome, Lyon [Phys. Fl. **28**, 338 (1985)] Monte Carlo code
 - Recently added global full radius particle distributions
- Various fast ion populations
 - ICRF tails (quasilinear diffusion operator)
 - Alphas
 - Neutral beam ions (pencil beam approximation)
 - Alfvén turbulence (to be added)
- Options for f and f particle weightings
- Diagnostics: particle and energy losses, loss patterns, energy slowing down, escaping pitch angle/energy/lifetime distributions
- Longer term goal: Multi-species (thermal, fast ion, impurity), coupled transport and electric field evolution model

Hamiltonian Guiding Center Orbit Equations:

$$\dot{\theta} = \frac{g}{D} \dot{P}_\perp - \frac{I}{D} \dot{P}_\parallel \quad \dot{P}_\parallel = \frac{1}{g} (\dot{P}_\perp + \dot{\theta}) - (P_\perp + I) \frac{g}{g^2} \dot{\theta} - \dot{\theta}$$

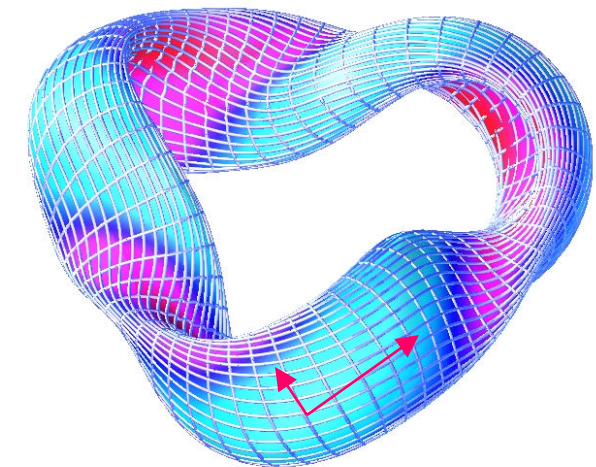
$$\dot{P}_\perp = \frac{e^2 c^2 B}{m} \frac{B}{m} + \frac{e^2 c B^2}{m} \frac{c}{m} + \mu \frac{B}{m} + e \frac{B}{m} - \frac{e^2 B^2}{m} \frac{c}{m} \frac{c}{P}$$

$$\dot{P}_\parallel = \frac{e^2 c^2 B}{m} \frac{B}{m} + \frac{e^2 c B^2}{m} \frac{c}{m} + \mu \frac{B}{m} + e \frac{B}{m} - \frac{e^2 B^2}{m} \frac{c}{m} \frac{c}{P}$$

where $D = gq + I + \frac{c}{m} (gI - Ig)$

$$\dot{P}_\perp = -\frac{B}{m} \frac{e^2 c^2 B}{m} + \mu - \frac{e^2 c B^2}{m} \frac{c}{m} - e \frac{B}{m}$$

$$\dot{P}_\parallel = -\frac{B}{m} \frac{e^2 c^2 B}{m} + \mu - \frac{e^2 c B^2}{m} \frac{c}{m} - e \frac{B}{m}$$

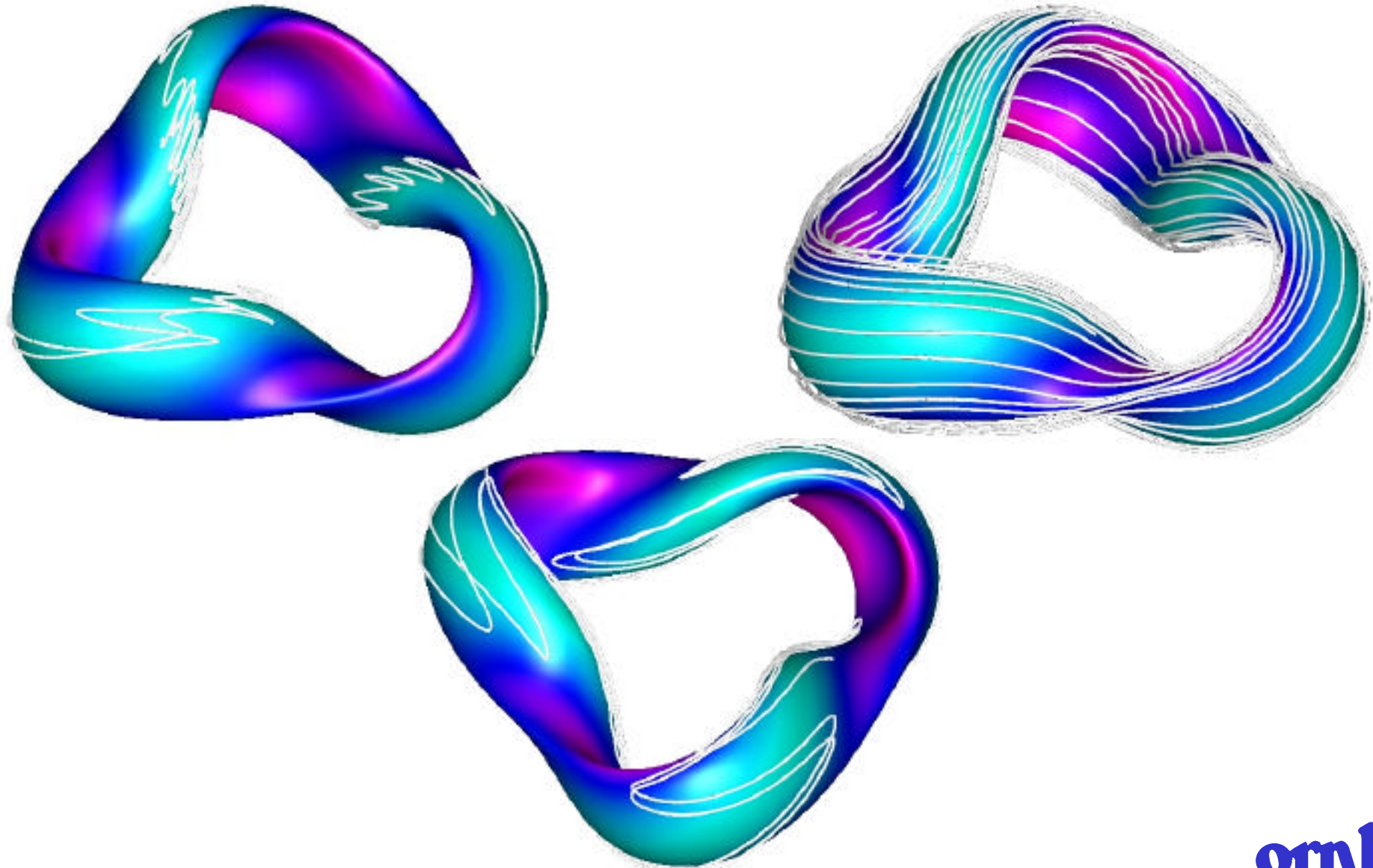


Perturbed fields (e.g., from an AE instability) are introduced from:

and $\vec{B}' = \vec{B} \times \vec{B}$, $= \sum_{m,n} [A_{mn}(t), B_{mn}(t)] e^{i(n-m-t)}$

[Ref.: R. B. White, Phys. Fl. **B** 2 (1990) 845]

Our model follows non-interacting particle trajectories through 4D phase space colliding with a static background plasma modeled with a 2D velocity space Monte Carlo diffusion operator



Coulomb collision operator for collisions of test particles (species a) with a background plasma (species b)

Ref. S. P. Hirshman, D. J. Sigmar, Phys. Fl. **19** (1976)

$$C_{ab} f_a = \frac{D^{ab}}{2} - (1 - \frac{v^2}{v_b^2}) \frac{f_a}{v} + \frac{1}{v^2} \frac{v^2 - v_b^2}{v} \frac{2}{v} \frac{\partial}{\partial v} f_a + \frac{3}{v} \frac{\partial^3}{\partial v^3} \frac{f_a}{v}$$

where

$$\frac{D^{ab}}{D^0} = \frac{\int_0^{v_b}}{(v/v_b)^3} \left(\frac{v}{v_b} - G \right) \frac{v}{v_b} = \frac{G^{ab}}{G^0} \frac{v}{v_b}$$

$$(x) = \frac{2}{\sqrt{\pi}} \int_0^x dt t^{1/2} e^{-t} \quad G(x) = \frac{1}{2x^2} [(x) - x (x)]$$

$$\frac{v_b}{v_{b0}} = \sqrt{\frac{2T_{b0}}{m_a}} \quad \frac{v}{v_b} = \sqrt{\frac{2T_{b0}}{m_b}} \quad \frac{G^{ab}}{G^0} = \frac{4 n_b \ln(\frac{e_a e_b}{v_b v_{b0}})}{(2T_b)^{3/2} m_a^{1/2}}$$

Monte Carlo Equivalent of the Fokker-Planck Operator

[A. Boozer, G. Kuo-Petravic, Phys. Fl. **24** (1981)]

$$n = n_{-1} \left(1 - \frac{d}{d} t \right) \pm \left[\left(1 - \frac{2}{n_{-1}} \right) \frac{d}{d} t \right]^{1/2}$$

$$E_n = E_{n-1} - (2 - t) E_{n-1} - \frac{3}{2} + \frac{E_{n-1}}{dE} d T_b \pm 2 [T_b E_{n-1} - t]^{\gamma/2}$$

Local Monte-Carlo equivalent quasilinear ICRF operator (developed by J. Carlsson)

$$E^+ = E^- + \mu^E + \sqrt{\epsilon_{EE}}$$

ϵ = a zero – mean, unit – variance random number (i.e., $\mu = 0$ and $\sigma = 1$)

$$\epsilon_{EE} = 2m^2v^2 - v_0^2 = 2 \left(\frac{k_{\parallel}v_{\parallel}}{v^2} - \frac{v_{\parallel}^2}{v^2} \right)^2 \frac{v^3}{v^2} v_0^2$$

$$\mu^E = 2 \left(1 - \frac{k_{\parallel}v_{\parallel}}{mv} \right) v_0 \quad \mu = 2 \left(1 - \frac{k_{\parallel}v_{\parallel}}{v^2} \right) \frac{k_{\parallel}}{v^2} - \frac{v_{\parallel}^2}{v^2} + \frac{v_{\parallel}v^2}{v^2} \frac{v}{v_0}$$

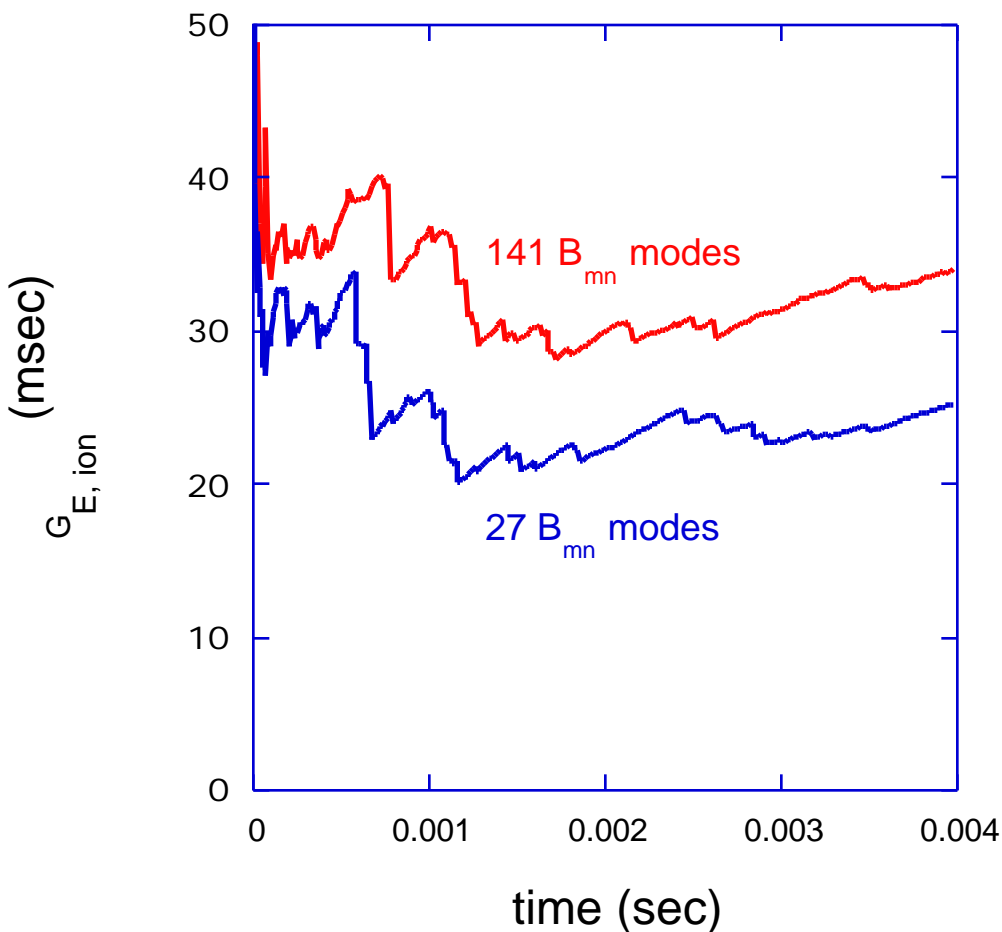
where

$$v_0 = \frac{1}{v} \frac{eZ}{2m} |E_+ J_{n-1}(k_{\parallel}) + E_- J_{n+1}(k_{\parallel})|^2 \frac{2}{n|J|}$$

as $k_{\parallel} \rightarrow 0$

$$\frac{2}{n|J|} \rightarrow 2^{-2} \left| \frac{2}{n|J|} \right|^{2/3} \times Ai^2 \left(-\frac{n^2}{4} \left| \frac{2}{n|J|} \right|^{4/3} \right)$$

Performance issues in applying DELTA5D code to QOS



- Used routinely in parallel mode on the SGI/Cray T3E - MPI
- Scalable up to 512 processors
- Global transport studies of QOS devices can require 100 - 200 B_{mn} 's for good convergence
- CPU time for particle simulations scales linearly with # of B_{mn} 's
- 3D spline representation of $B(. , .)$ offers a factor of 10 - 15 speedup over direct summation of the Fourier series.

Recent full radius particle transport simulations show that QOS neoclassical energy lifetimes (for $R_0/\langle a \rangle = 3.6$) exceed ISS95 by a factor ranging from 2 - 5 depending on density and temperature.

- 32768 particles distributed over cross-section

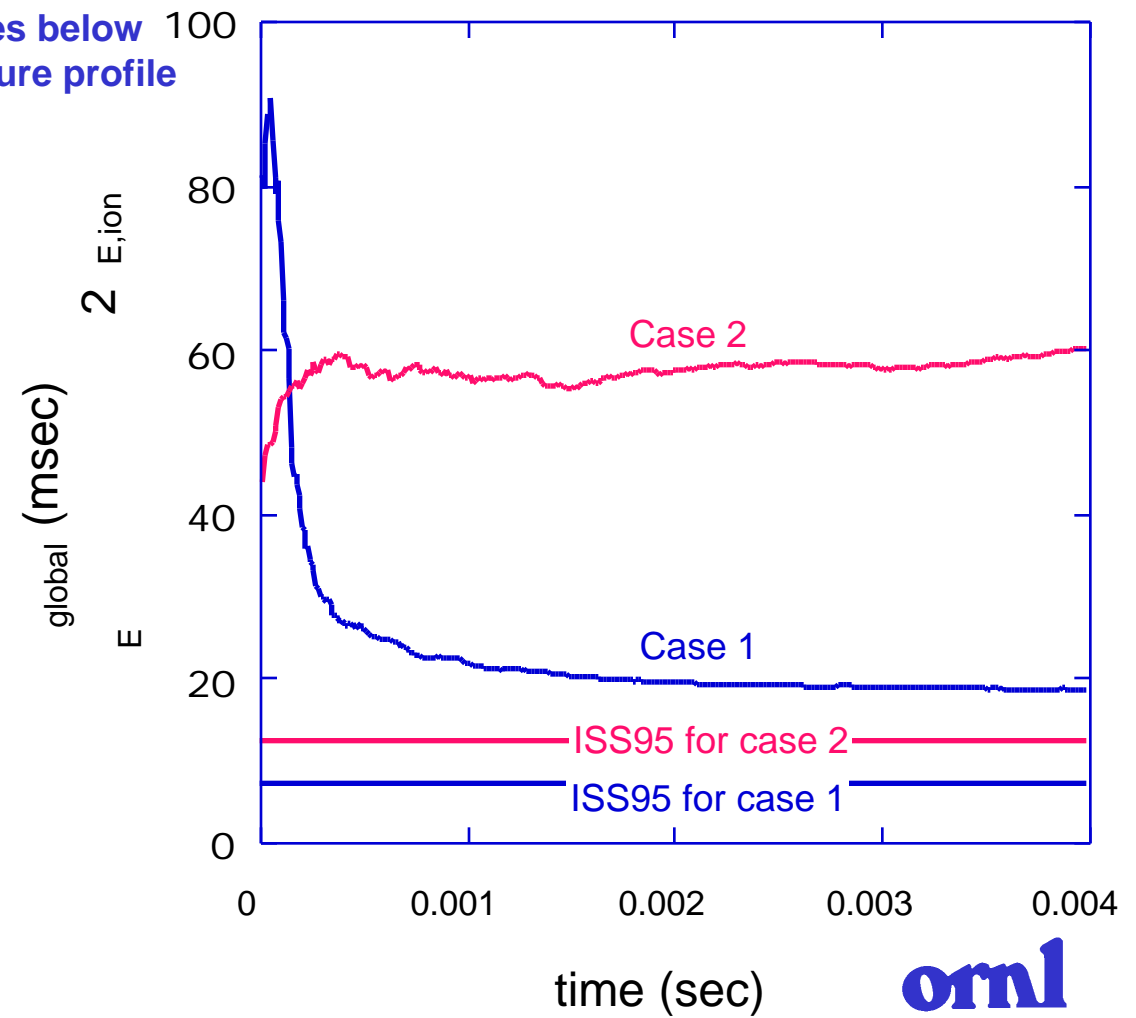
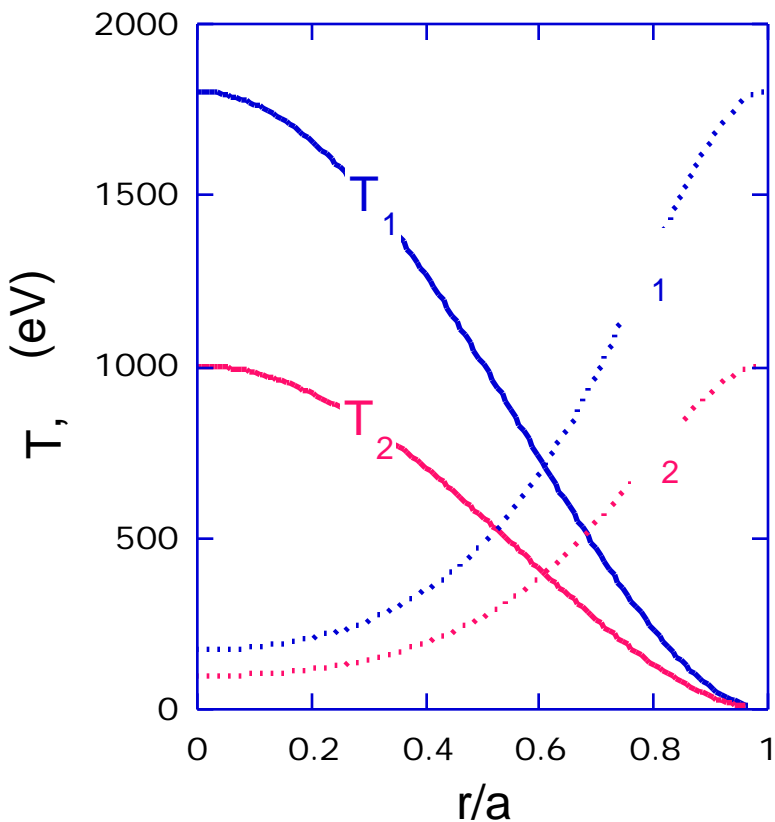
- $E_{\text{ion}}^{\text{ion}}$ = global ion energy lifetime

- Particle reseeding: $n = \text{constant}$, $T = \text{profiles below}$

- $T_i = T_e$, $Z_{\text{eff}} = 1$, parabolic squared temperature profile

- case 1: $n(0) = 3 \times 10^{13} \text{ cm}^{-3}$, $T(0) = 1.8 \text{ keV}$

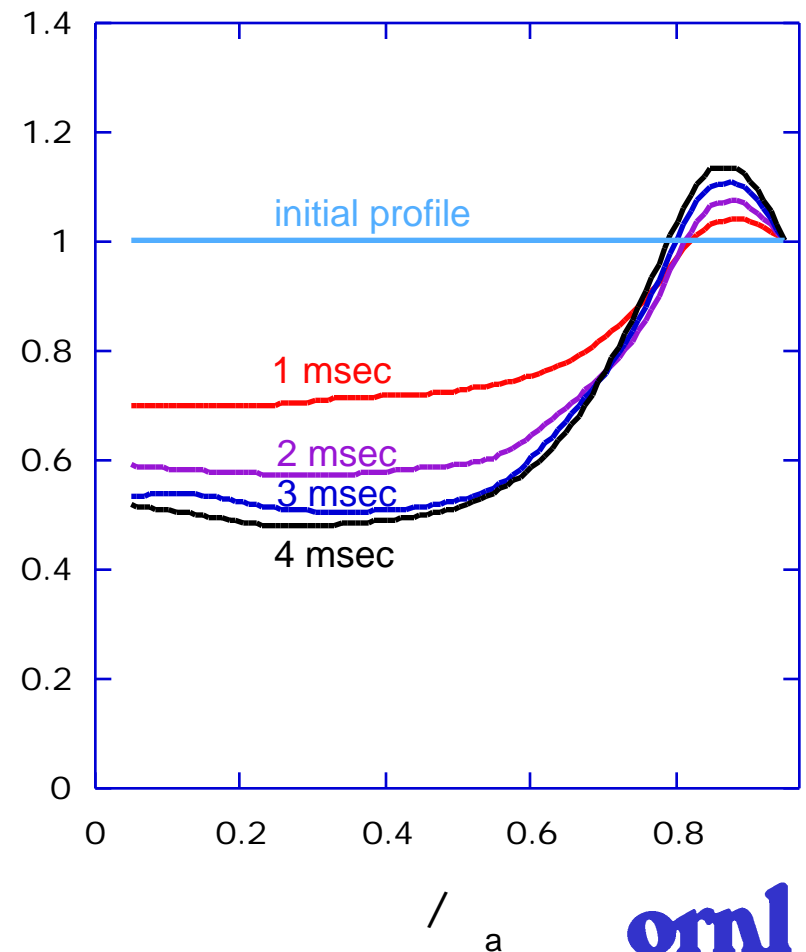
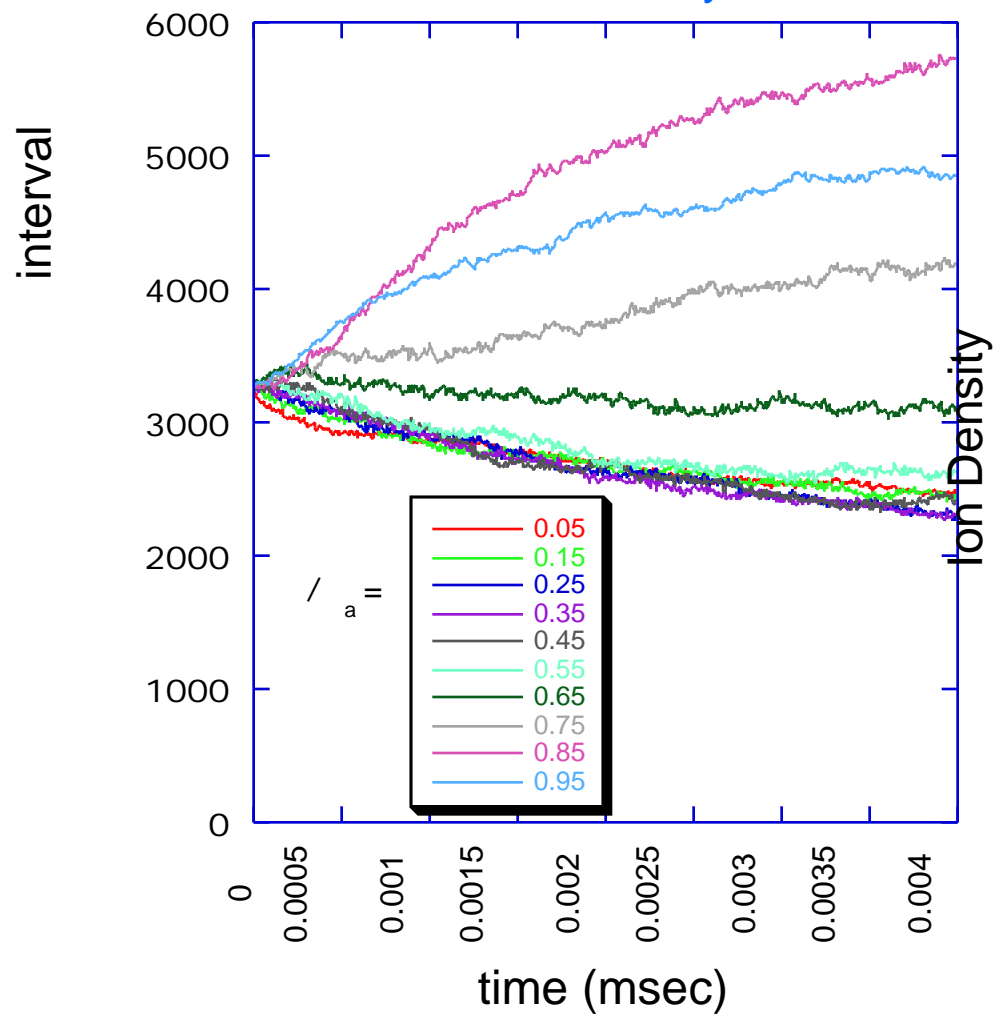
- case 2: $n(0) = 9 \times 10^{13} \text{ cm}^{-3}$, $T(0) = 1 \text{ keV}$



For the low density, higher temperature case, the ion particle density evolves to a hollow profile shape.

In future work will explore dependence on:

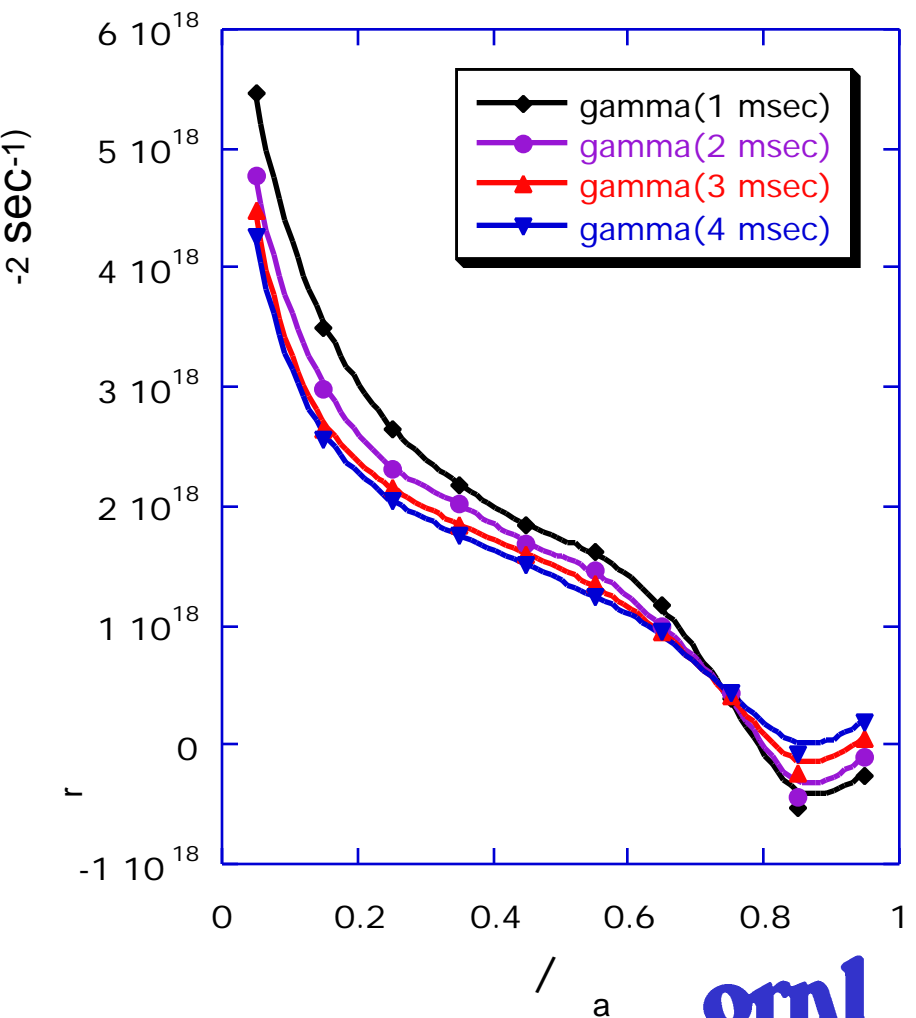
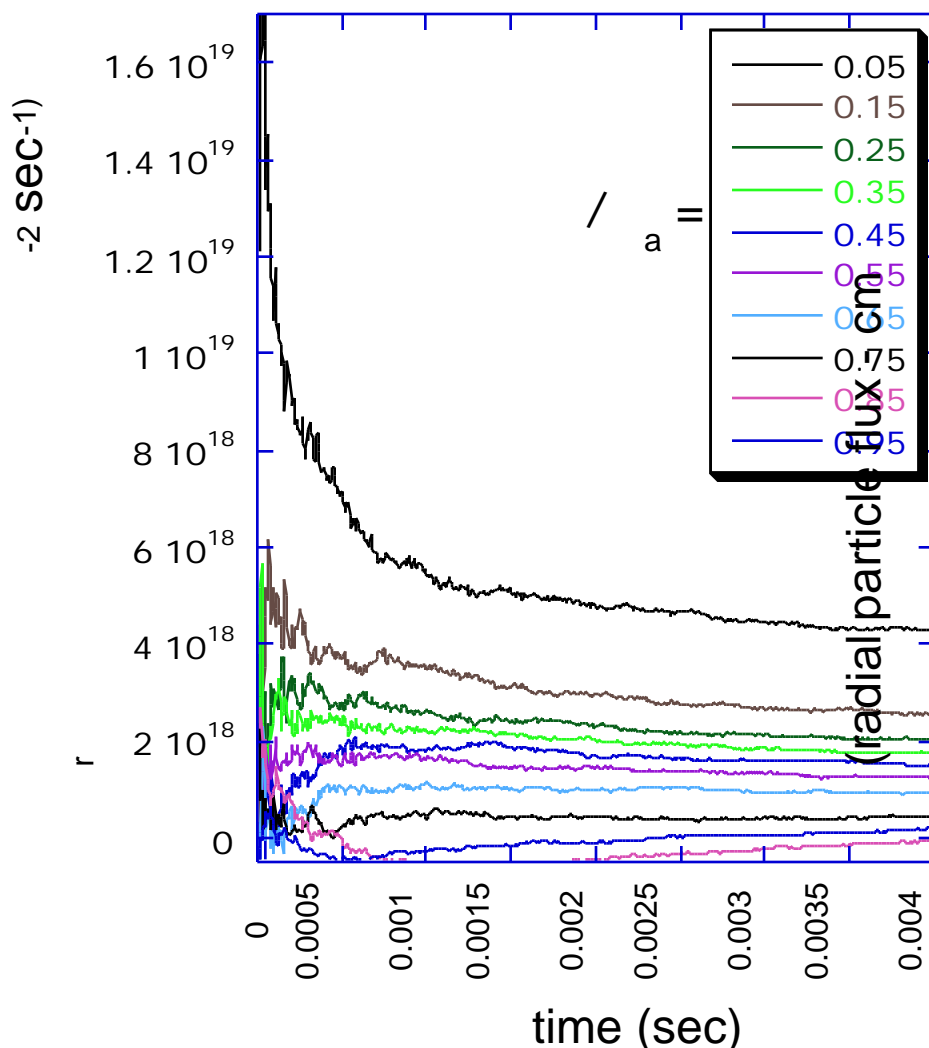
- Particle refueling and energy input model
- Self-consistency between collision operator and particle profiles



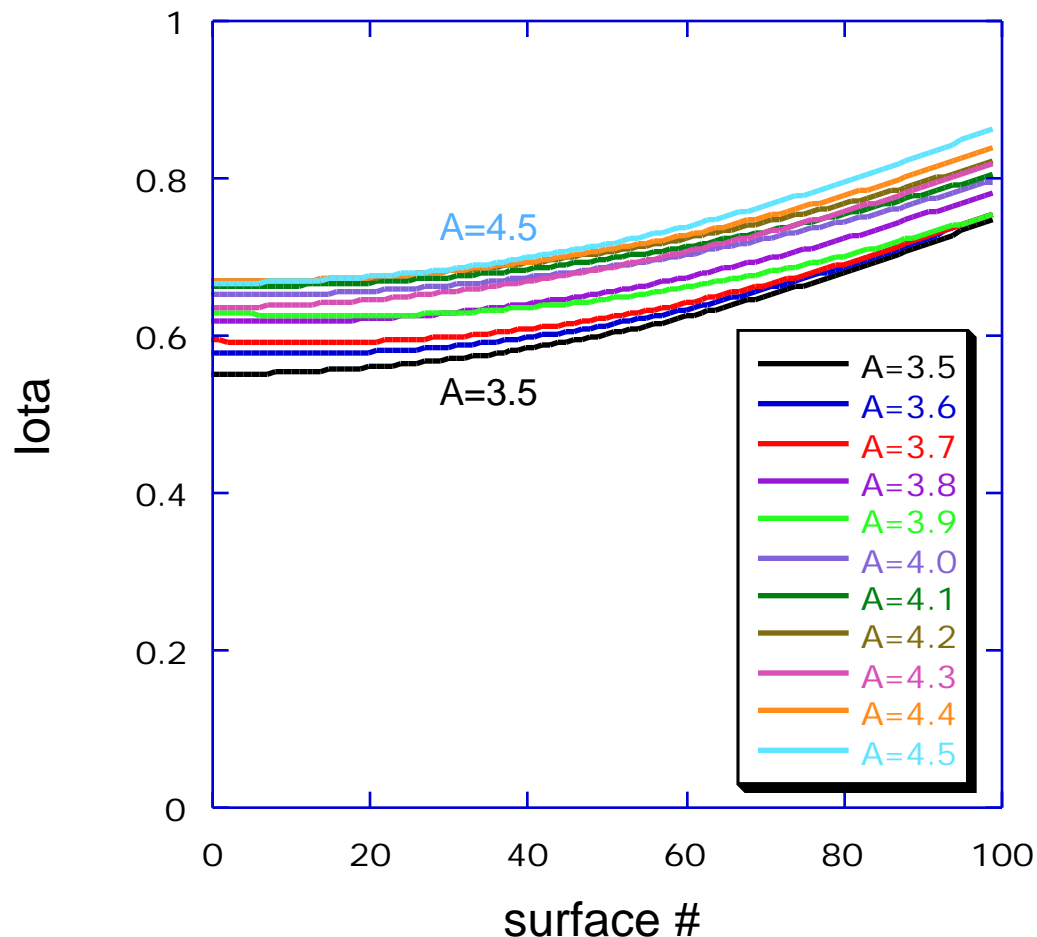
Particle fluxes are peaked near the center
where the ion temperature is highest

$$n(0) = 3 \times 10^{13} \text{ cm}^{-3}, T(0) = 1.8 \text{ keV}$$

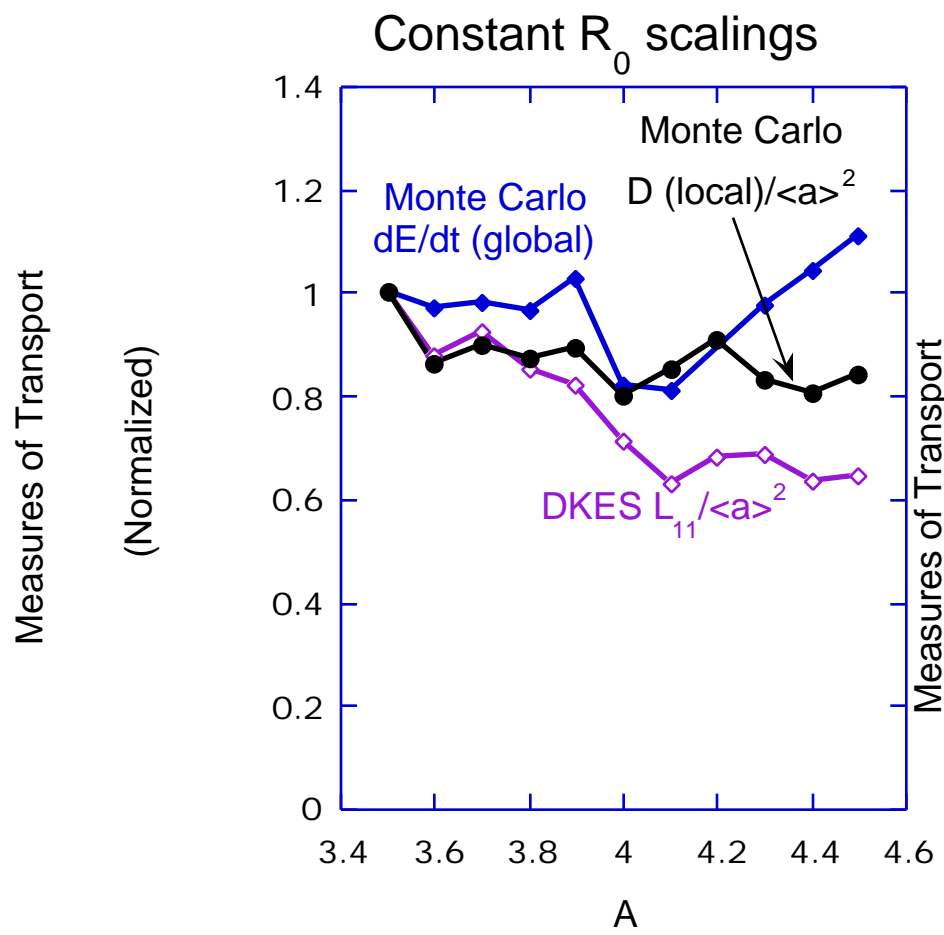
time-averaged ion particle fluxes



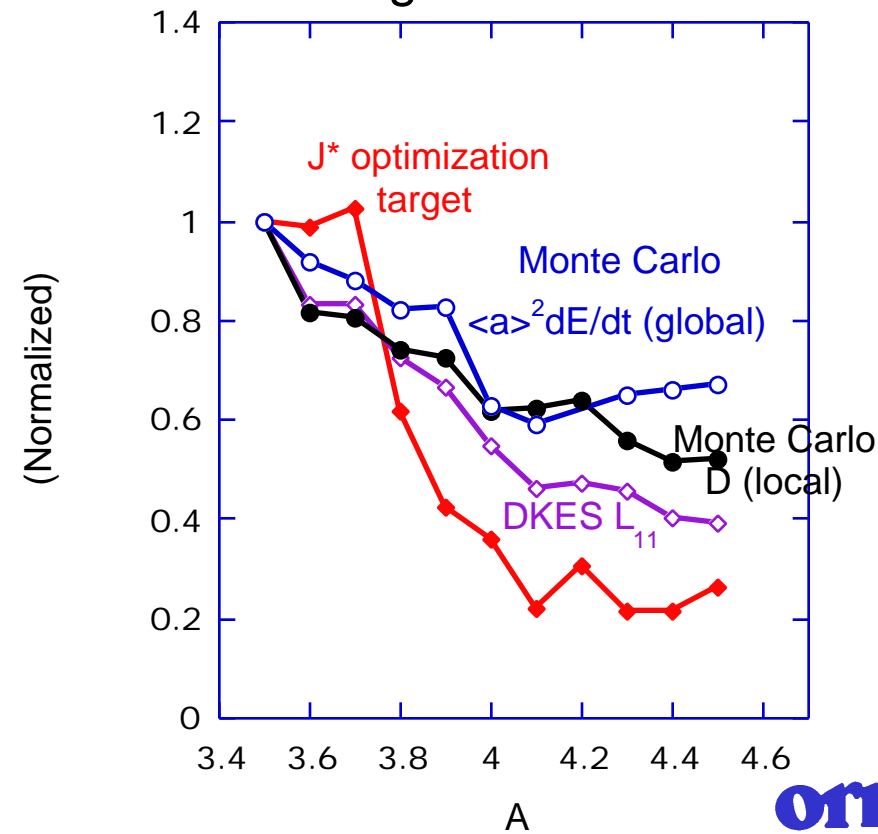
Recent QOS designs have focused on
the aspect ratio scans in the range of
 $R_0/\langle a \rangle = 3.5$ to 4.5



Transport studies show that relatively uniform degrees of optimization can be achieved at constant R_0 in this range of A's. (Future studies also need to look at constant aR_0 - i.e., constant cost)

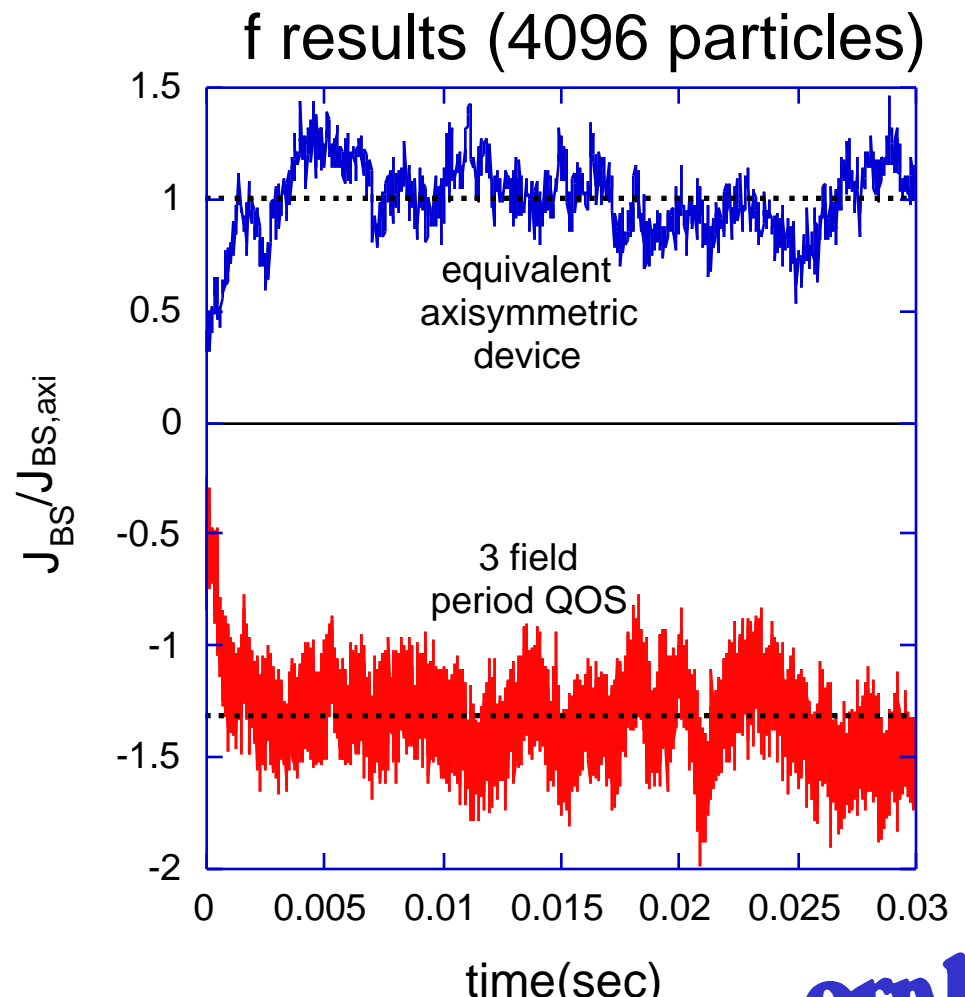
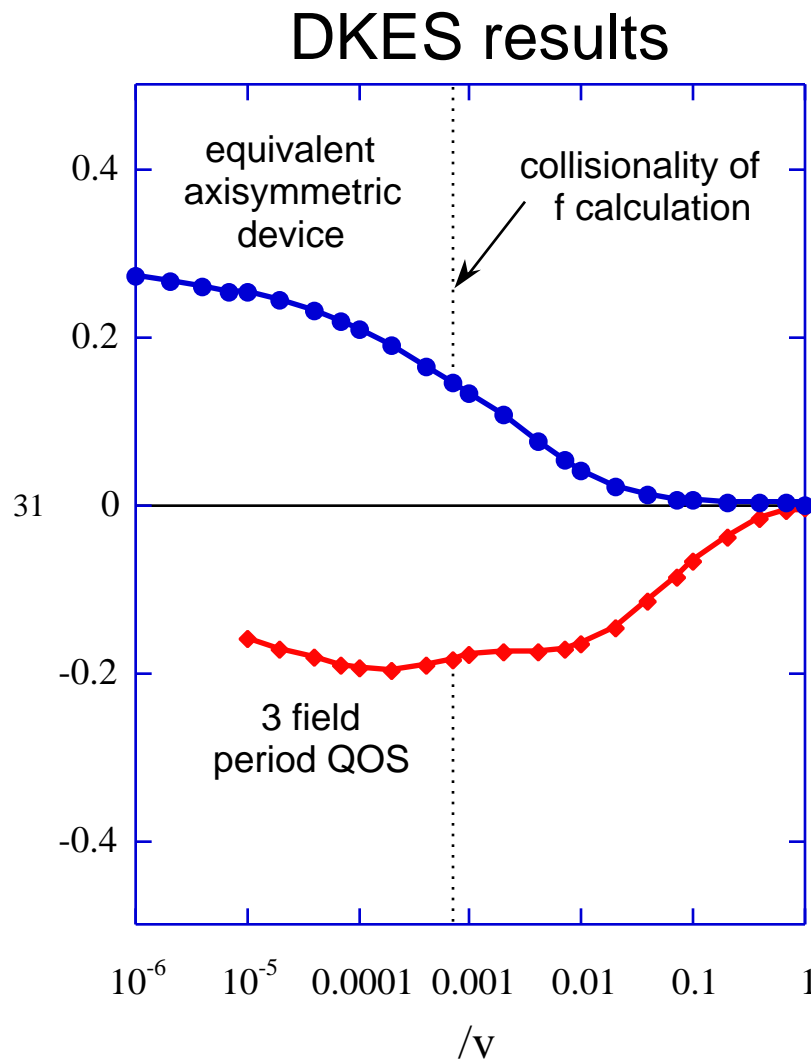


- Removing $\langle a \rangle^2$ size scaling effect indicates effectiveness of J^* target function



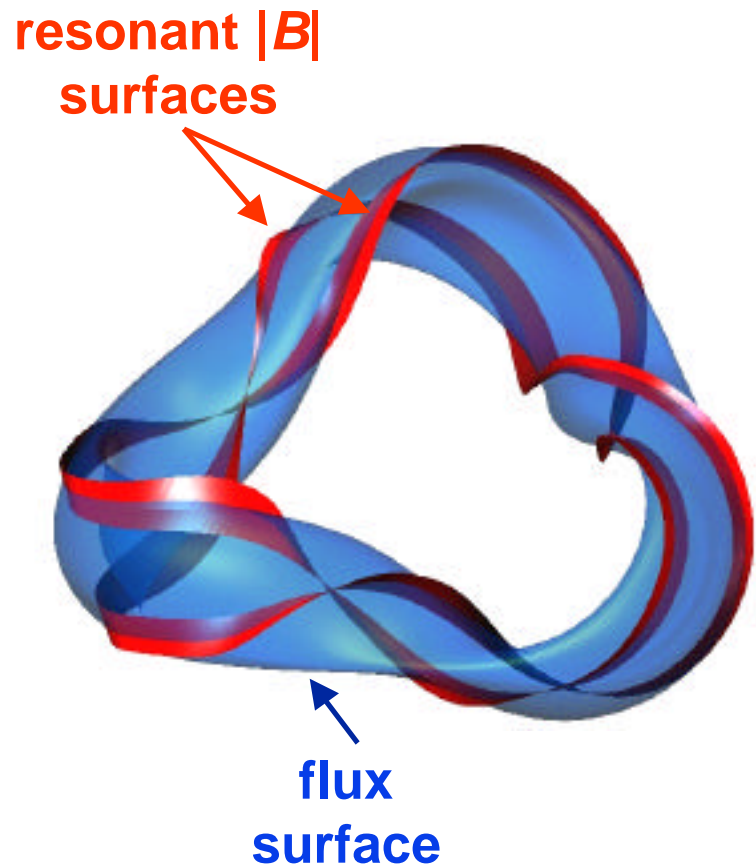
Bootstrap current levels for a QO device and its axisymmetric equivalent show agreement between DKES and the f particle code:

$(J_{BS}^{\text{non-axi}}/J_{BS}^{\text{axi}} = -1.309 \text{ from DKES and } = -1.32 \text{ from } f)$



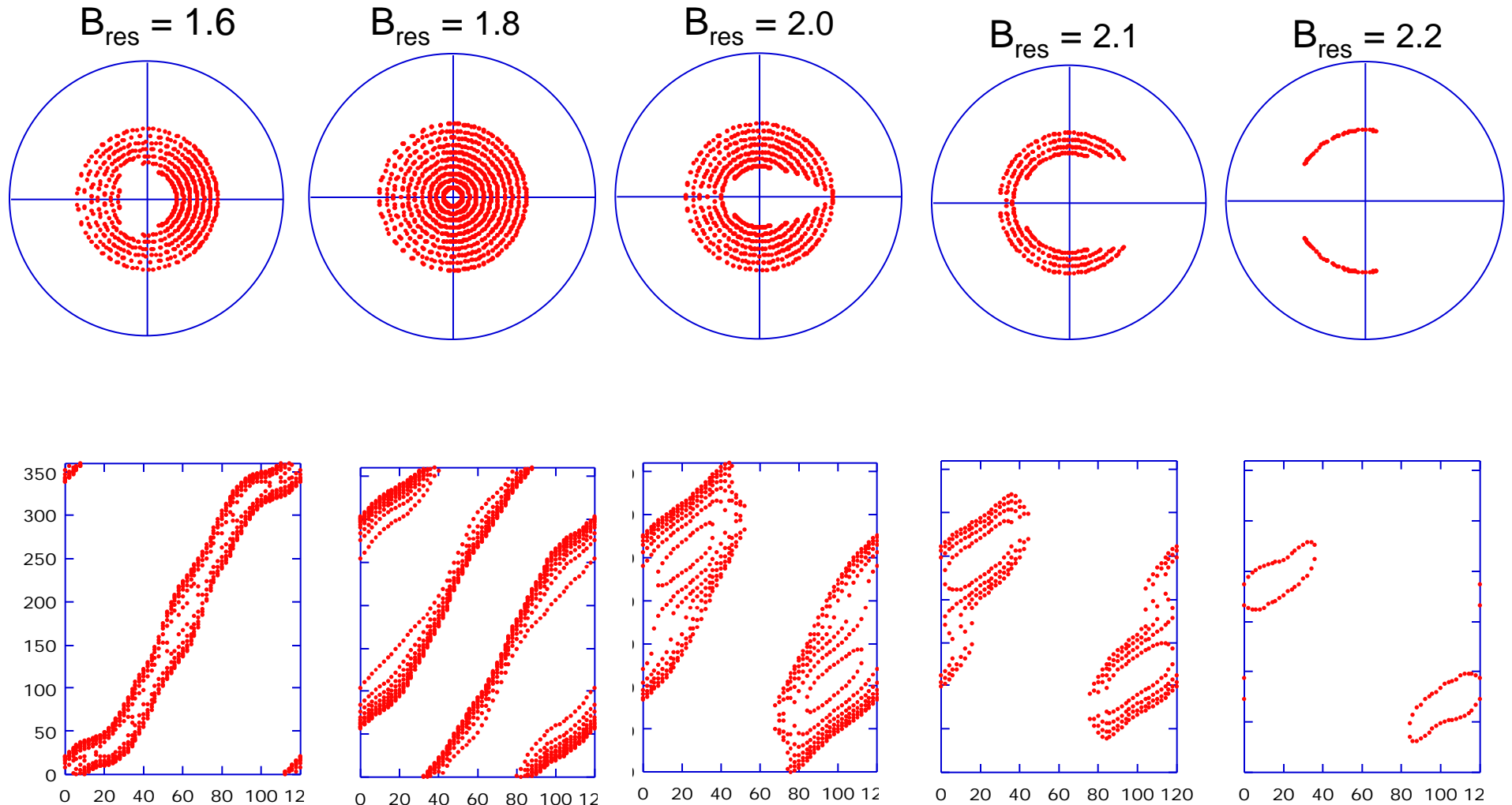
Monte Carlo Calculations Used to Assess Energetic Ion Losses and ICRF Heating

- Quasi-linear ICRF diffusion operator (follows particles as they are kicked up in energy)
 - Intersections of $|B|$ contours with flux surfaces determined
 - Ions are started out at $B = B_{\text{res}}$ with $v_{||0}/v = 0$ (equivalent to $\mu/B = B_{\text{res}}$)
- Simple RF wave-field model:
 $k_{||} = n/2 R_0$, $n = 1$, $k_{\perp} = 0$
 $E_+ = E_+^0 \exp[-(r - 0.3)^2]$, $E_- = 0$
- Eventual goal is to incorporate particle simulation model with ORNL RF Full Wave codes



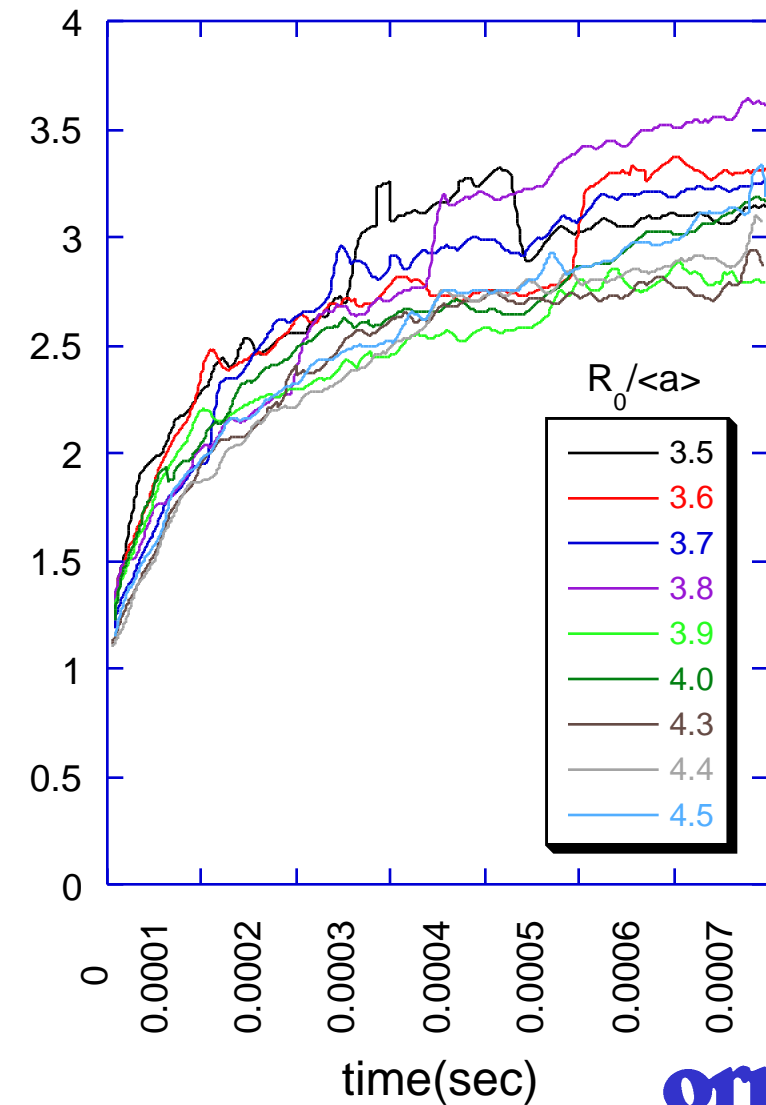
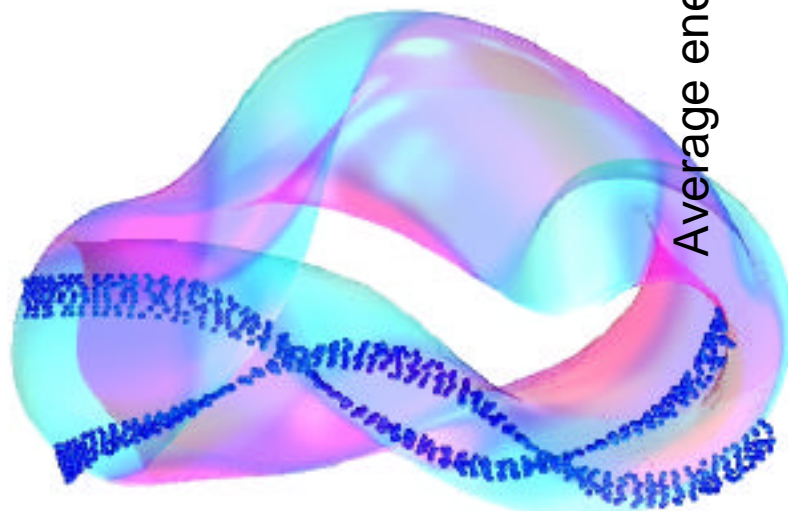
ICRF resonance locations for different heating frequencies

(top figures - projected onto fixed toroidal plane
bottom figures - up to 10 flux surfaces projected onto a ϕ , θ plane)

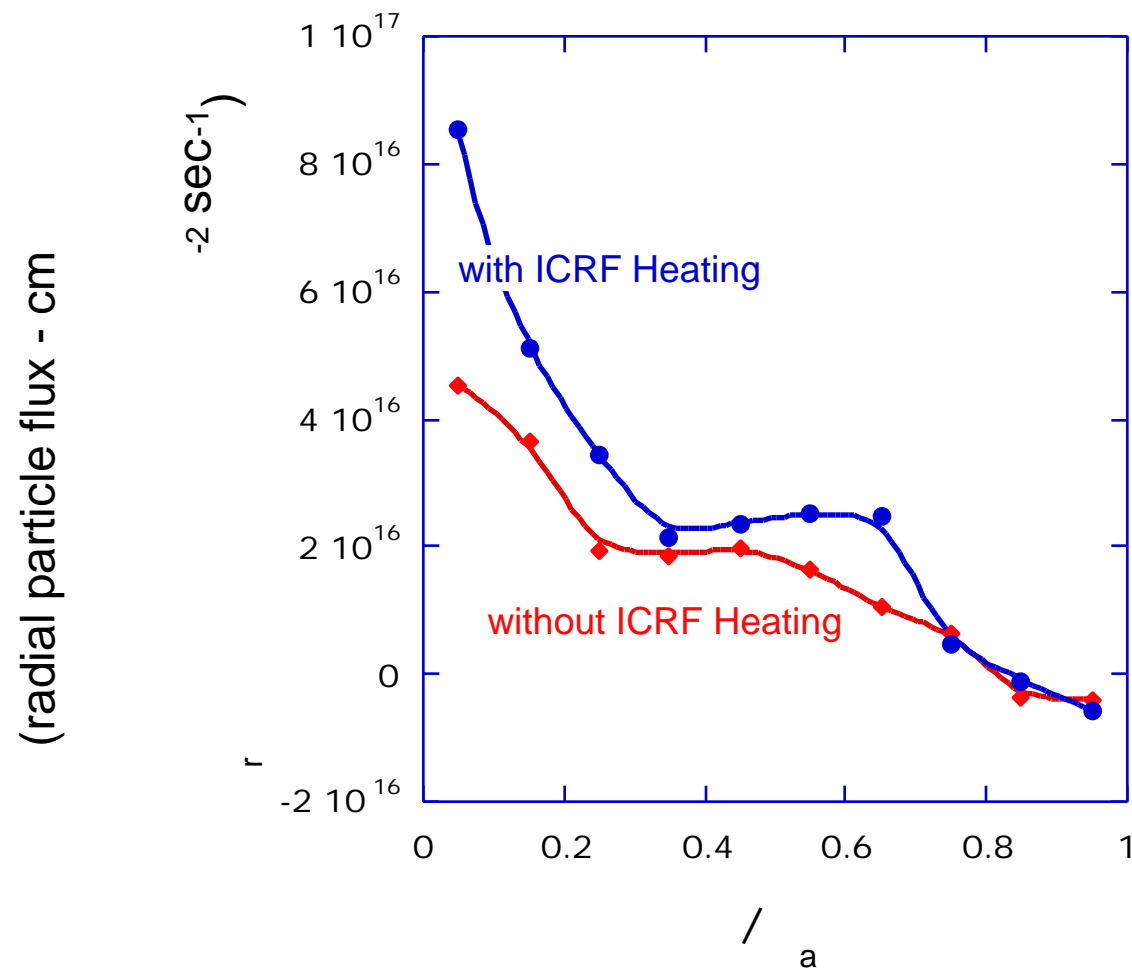


Initial particle simulations of ICRF absorption show ion confinement is adequate for heating.

- 1024 ions followed with:
 - Coulomb collisions with background ions, electrons
 - RF heating operator
- Ions are initially loaded in at resonance locations with $v_{\parallel 0}/v_0$ (see below)

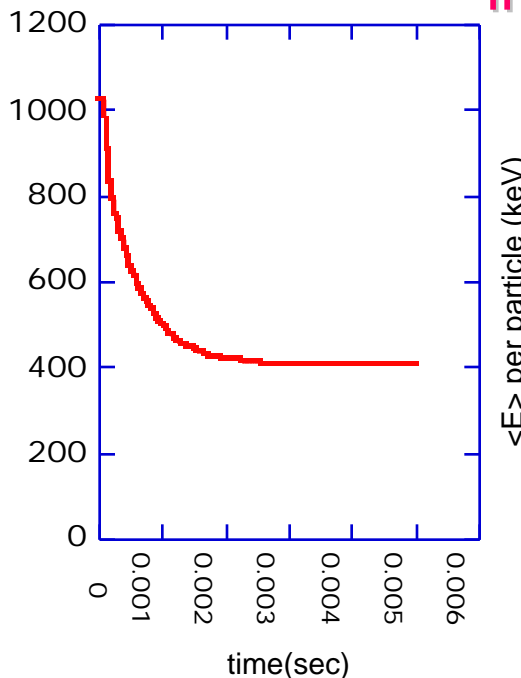


Since ICRF heating does not preserve μ or J , it can enhance radial particle fluxes. This can be an important issue and control knob for the generation of the ambipolar electric field

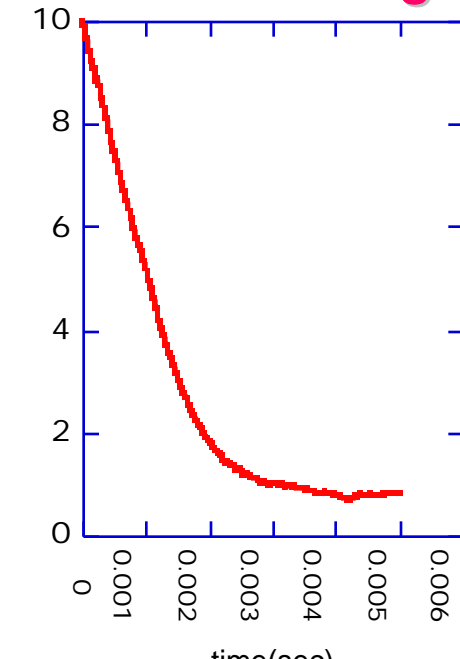


Confined and escaping ion diagnostics are tracked in our ICRF heating model:

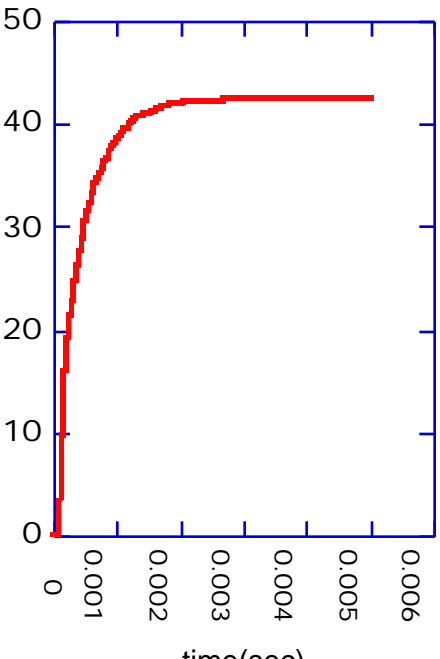
of confined particles



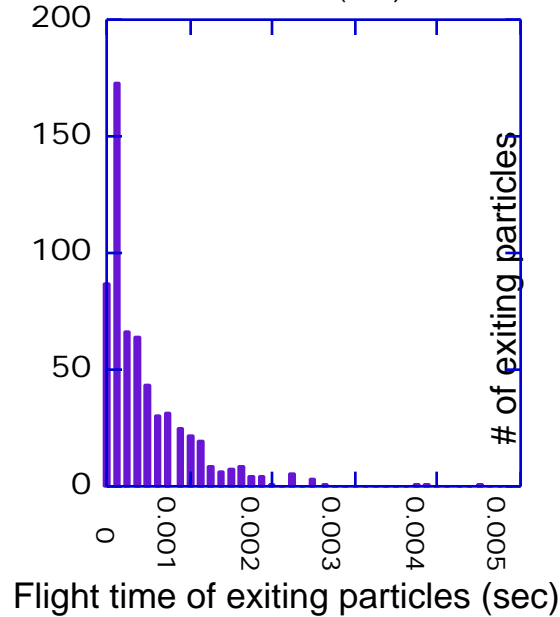
$\langle E \rangle$ per particle (keV)



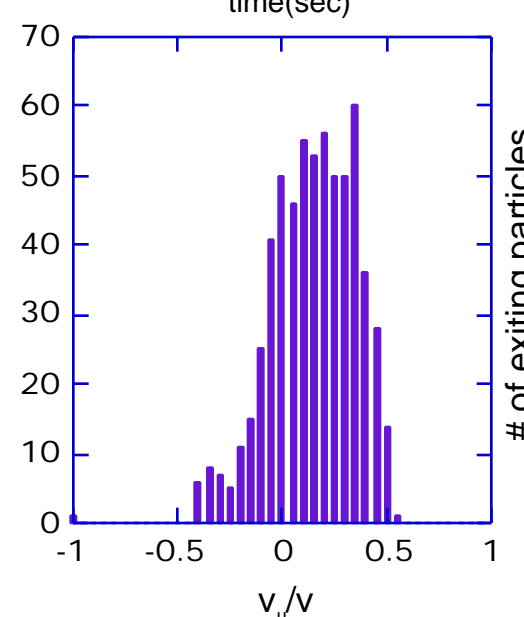
% Energy losses



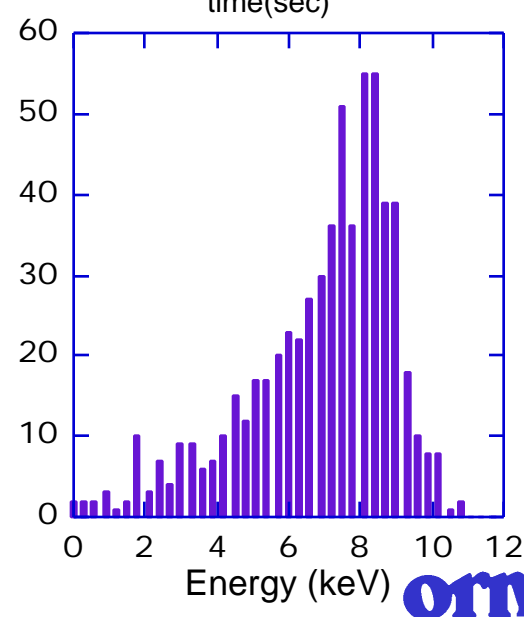
of exiting particles



of exiting particles



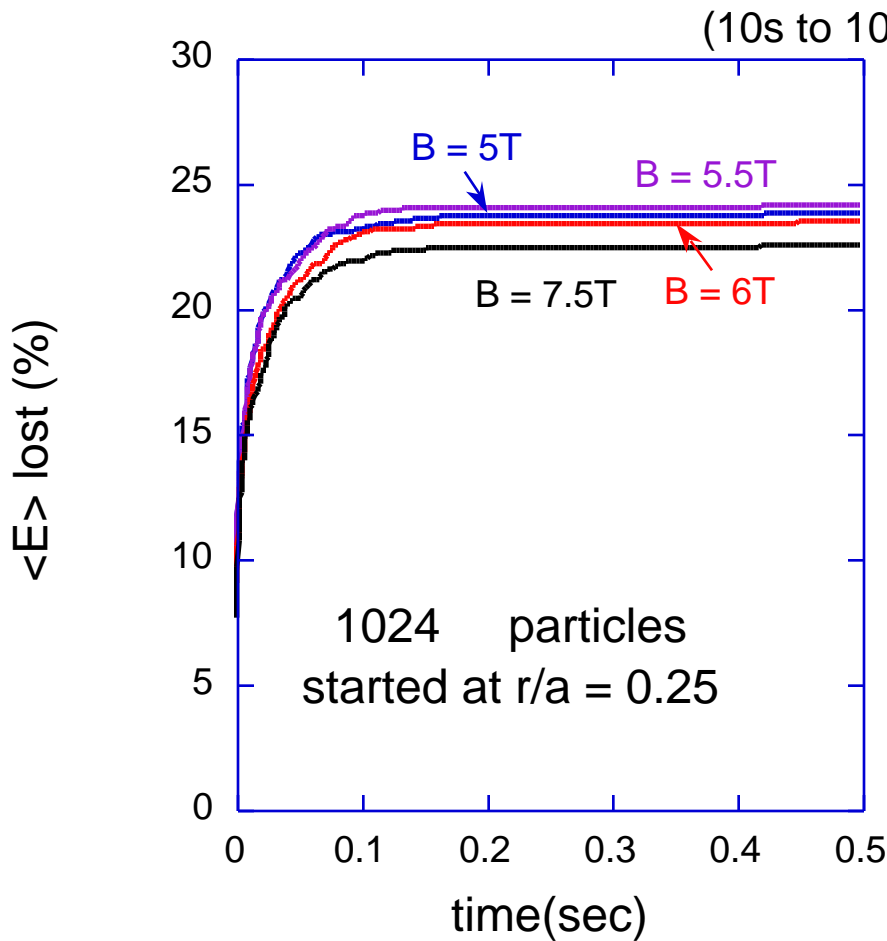
of exiting particles



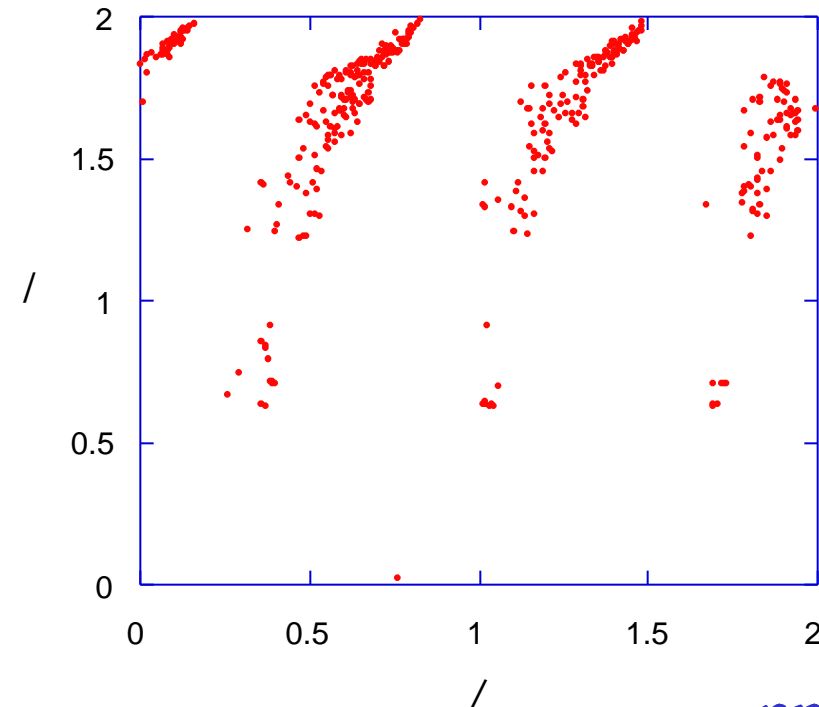
ornl

Although QO devices have not yet been specifically optimized for a reactor, they achieve levels of alpha losses which are adequate for fusion power balance

- Alpha slowing-down in a QO stellarator reactor (time scale disparity: bounce time 1 μ second, slowing-down time 0.2 - 1 second)
- Alpha slowing-down simulations in stellarators require T3E level performance



Alpha loss locations on outermost closed flux surface

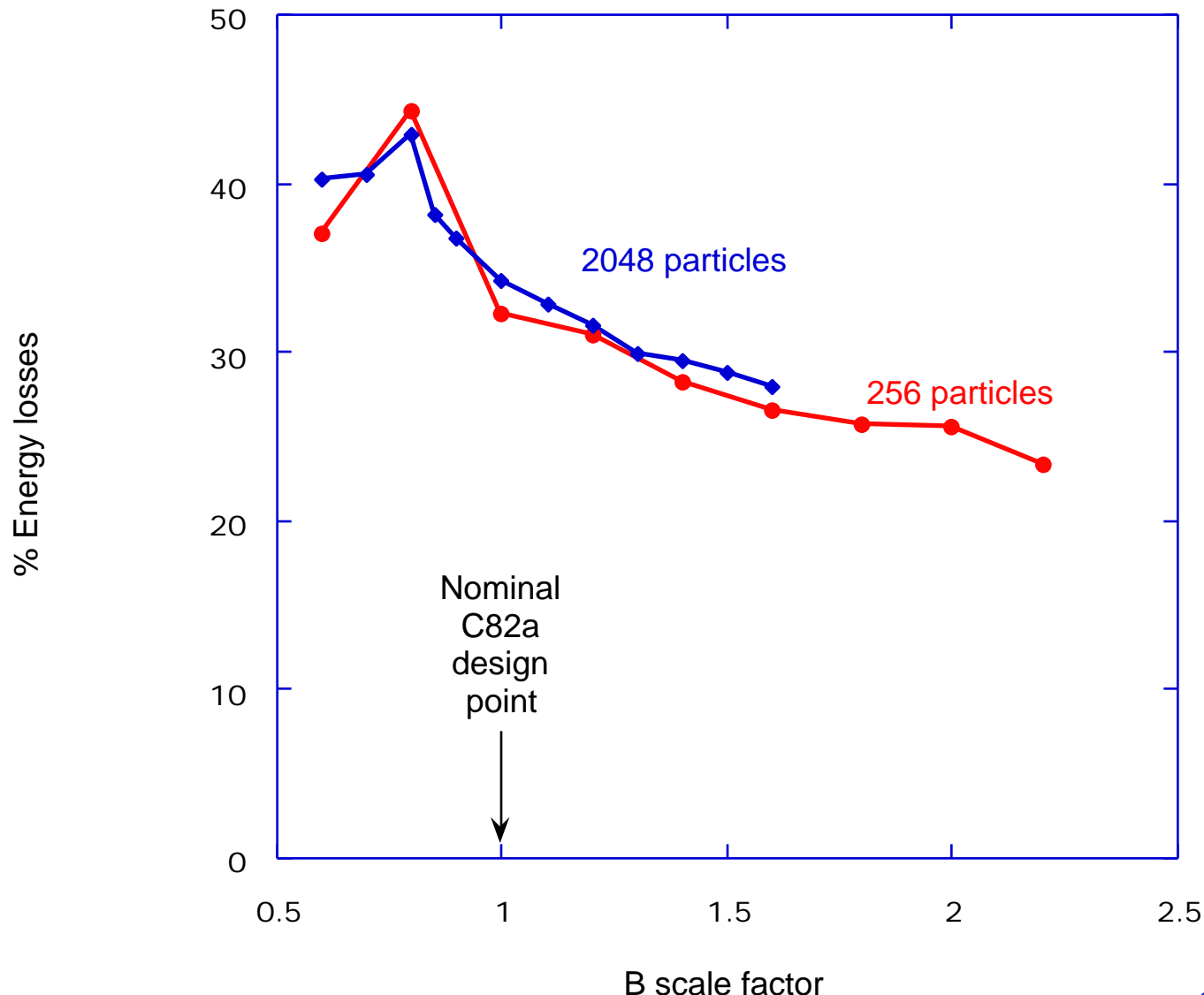


Neutral Beam Heating Model

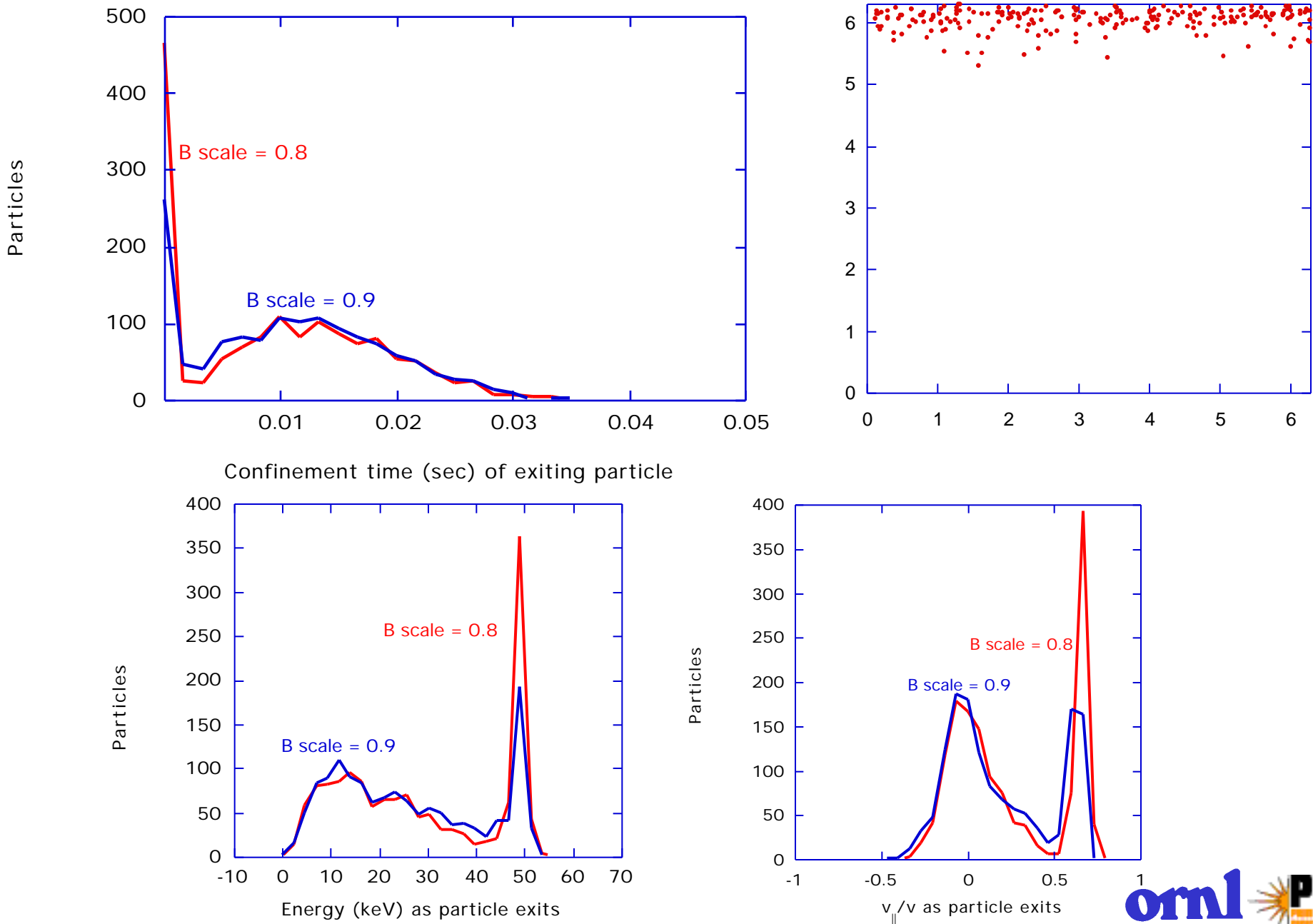
(M. Zarnstorff, M. Redi)

- Applied only to Quasi-axisymmetric PoP devices
- Uses a prescribed beam ionization/deposition profile obtained from TRANSP for initial conditions
- Follows an ensemble of orbits through several slowing-down times and records
 - time variation of average energy
 - energy losses through outer flux surface and loss patterns on outer surface
 - histograms of confinement time, energy, pitch angle of lost particles
 - merges beam particles in with thermal population when they reach $3/2 kT_{ion}$

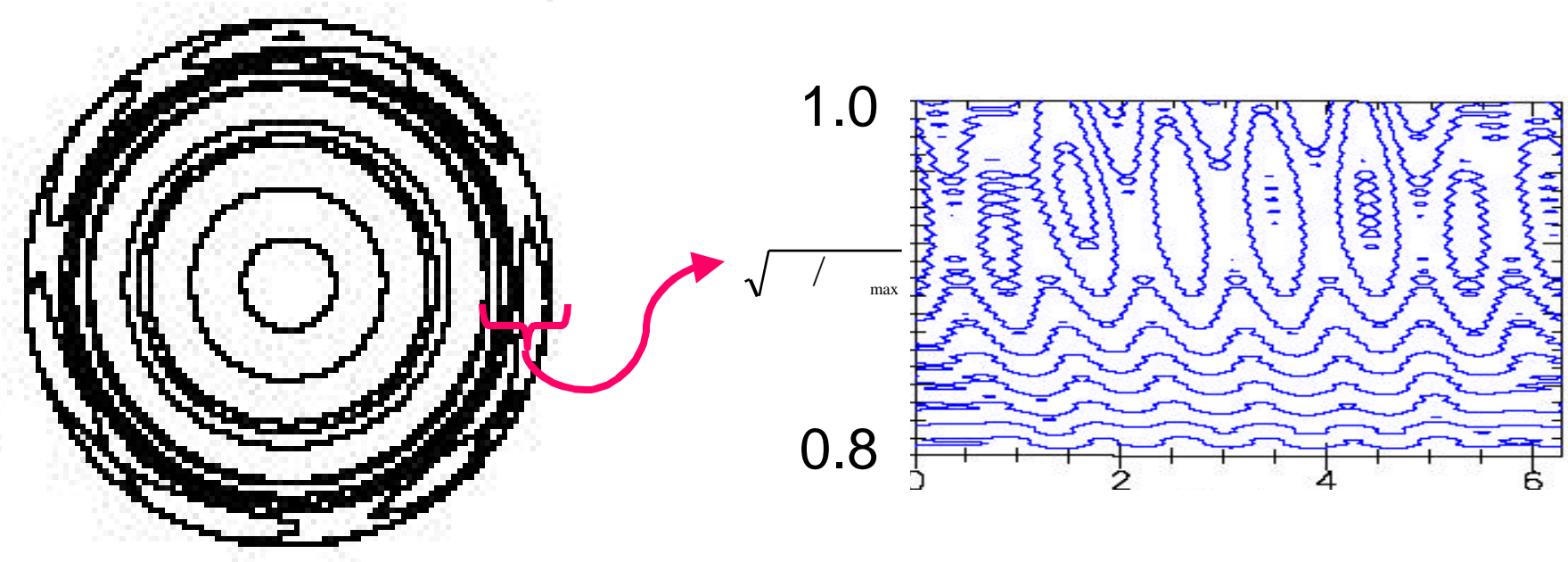
NBI losses in c82a at 50 keV injection energy



Escaping NBI Particle Histograms



Preliminary calculations of $J \circ v_{\parallel} dl$ contours for 5 - 50 keV barely passing particles in QA devices show loss regions at the plasma edge:



- Inclusion of J (in the plasma edge region) as an optimization target could lead to improvements in beam ion confinement

CONCLUSIONS

- Unique features of QO devices
 - Low aspect ratio, good volume utilization
 - Bootstrap current < current required in tokamak for same transform
 - $i_{\text{Bootstrap}} \ll i_{\text{coils}}$ (i.e., transform comes predominantly from coils)
 - good test-bed for RF bulk heating
 - optimized for confinement of high v trapped particles
 - high field access
 - can be designed to access $0.5 < i < 0.8$
- Confinement evaluations of QO configurations
 - DKES provides neoclassical transport matrix for full mixed helicities
 - With spectral optimization - good convergence for QO parameters
 - Applications: bootstrap current, ambipolar electric field models, viscosities
 - DELTA5D particle code: thermal and fast ion transport physics
 - global thermal confinement can be a factor of 2-5 above ISS95
 - ICRF heated supra-thermal ions modify fluxes - influence electric field
 - Bootstrap currents agree with DKES
 - Next steps: ambipolar electric field, improve transport targets, self-consistency between test and field particle models, new f approaches